Residual strain measurements in InGaAs metamorphic buffer layers on GaAs

V. Bellani[1,a], C. Bocchi[2], T. Ciabattoni[1], S. Franchi[2], P. Frigeri[2], P. Galinetto[1], M. Geddo[3], F. Germini[2],
G. Guizzetti[1], L. Nasi[2], M. Patrini[1], L. Seravalli[2], and G. Trevisi[2]

[1] Dipartimento di Fisica "A. Volta" and CNISM, Università di Pavia, 27100 Pavia, Italy
[2] CNR-IMEM Institute, Parco delle Scienze 37a, 43100 Parma, Italy
[3] Dipartimento di Fisica and CNISM, Università di Parma, 43100 Parma, Italy

Abstract. This work deals with the strain relaxation mechanism in InGaAs metamorphic buffers (MBs) grown on GaAs substrates and overgrown by InAs quantum dots (QD). The residual strain is measured by using Raman scattering and X-ray diffraction, both in Reciprocal Space Map and in single $\omega - 2\theta$ scan modes (ω and θ being the incidence angles on the sample surface and on the scattering planes, respectively). By relating the GaAs-like longitudinal optical phonon frequency ω^{LO} of InGaAs MBs to the in-plane residual strain ε measured by means of photoreflectance (PR), the linear ε-vs.-ω^{LO} working curve is obtained. The results of Raman and XRD measurements, as well as those obtained by PR, are in a very satisfactory agreement. The respective advantages of the techniques are discussed. The measurements confirm that strain relaxation depends on the thickness t of the buffer layer following a $\sim t^{-1/2}$ power law, that can be explained by an energy-balance model.

PACS. 78.30.Fs III-V and II-VI semiconductors – 61.10.-i X-ray diffraction and scattering – 71.70.Fk Strain-induced splitting

1 Introduction

Lattice strain in semiconducting materials is an effective tool to modify energy gaps, to shift and reverse the band edges of heavy-hole and light-hole bands, to remove band degeneracy at critical points of the Brillouin zone and to change band curvatures and hence-carrier effective masses [1,2]. The strain can be induced in a semiconductor by applying an external pressure or by epitaxially growing the material to be stressed on a lattice-mismatched substrate or layer that behaves as a virtual substrate. While the first approach is used to study the electronic band structure and related parameters, only the second one is suited for exploitation in devices. In this case, the structures may consist of a substrate, a buffer layer (termed as metamorphic buffer — MB) and the active part of the structure; by controlling the lattice parameter of the MB the mismatch between buffer and the upper part of the structure is changed and, hence, the strain in the active layer is affected. The lattice parameter of the MB depends on its composition and thickness through the mechanism of strain relaxation, by which — for MB thickness larger than a critical thickness — the elastic strain is partially relaxed and the formation of a network of misfit dislocations takes place.

The approach of engineering material properties by means of lattice strain has been used not only for semiconductors with a three-dimensional system of carriers, but also for quantum wells and superlattices (two-dimensional systems), quantum wires (one-dimensional systems) and quantum dots (zero-dimensional systems). Examples of structures that make use of MBs to improve device performances are: (a) high electron mobility transistor (HEMT) structures, grown on MBs to take advantage of the higher electron mobility and the better carrier confinement in the channel region made of In-rich InGaAs alloys [3]; (b) heterojuction bipolar transistor (HBT) structures prepared with base-layers of high In-content so as to have relatively small band gap and increased mobilities, saturation velocities, as well as reduced base contact-resistance [4]; and (c) multi-junction solar cells grown on MBs [5] that utilise a wider part of the solar spectrum, thus increasing the conversion efficiency. Also SiGe-based structures have taken and will take increasing advantages of strain engineering since the pioneering work of Abstreiter et al. [6] up to the most recent proposals [7].

In InAs/InGaAs QD structures light emission can be red-shifted to long-wavelengths ($\lambda \geqslant 1.3~\mu$m) [8–10] by QD strain engineering. In particular emission at 1.3–1.4 μm could be obtained at room temperature (RT) from InAs/InGaAs QDs by using the QD strain as a tuning parameter, which is controlled by the

---

[a] e-mail: `bellani@unipv.it`

thickness-dependent strain relaxation of suitably designed InGaAs MB [9,11,12]. Moreover, it has been shown that the QD strain engineering yields two degrees-of-freedom [13] that can be used not only to red-shift the emission, but also to enhance the RT emission efficiency, possibly up to 1.55 μm. Metamorphic buffers may have either constant composition or a continuously graded one; in the second case, in spite of the more sophisticated growth process that is required, advantage can be taken of the possibility to control the misfit dislocation distribution and of confining them close to the substrate-MB heterointerface — far from the active part of the structure — so that not to spoil its optoelectronic properties [14].

The use of strain to tailor the electronic properties of materials requires the capability of modelling strain relaxation and the availability of techniques to measure it in structures suited for specific applications, such as light-emitters.

Raman scattering has been usefully applied to measure the strain in InGaAs layers grown by different epitaxial techniques on GaAs or InP substrates [15–19]. These works have shown that the strain of an InGaAs layer can be derived by measuring the frequencies of the GaAs-like or the InAs-like optical phonon modes of the alloy.

Well-known and established X-ray diffraction methods [20,21] based on the measurement of asymmetric Bragg reflections both in linear scan mode and by reciprocal space mapping (RSM) allow the determination of the strain relaxation of mismatched heterostructures. By singling out the effects due to strain and to composition, the strain tensor components as well as the alloy composition can be obtained separately also for the general case of an arbitrary distortion of the epilayer lattice unit cell [22]. The main advantage of X-ray diffraction methods is the high accuracy in the measurements of lattice parameter a, with uncertainties $\Delta a/a < 1 \times 10^{-5}$.

In this work we present the investigation by micro-Raman scattering and by X-ray diffraction methods of strain relaxation in InGaAs metamorphic buffers incorporated in InAs/InGaAs QD nanostructures grown by Molecular Beam Epitaxy (MBE). The results show that the strain relaxation of MBs can be effectively predicted by the Marée et al. model [23] and that the strain can be measured in QD InAs/InGaAs structures for long-wavelengths operation at RT by means of the above mentioned techniques, the respective advantages of which are discussed. These results, along with those reported in reference [24], justify the approach of QD strain engineering [9,12,13] that may open the way to the fabrication of QD nanostructures for 1.55 μm operation at RT, a result of huge technological interest for telecom and datacom applications.

2 Experimental procedures

The structures grown on (100) GaAs substrates consist of: (i) a 100 nm-thick GaAs buffer layer; (ii) a $In_xGa_{1-x}As$ partially-relaxed metamorphic buffer MB (which acts also as lower confining layer (LCL) for QDs carriers) with thickness t ranging from 20 to 1000 nm and grown by MBE at 490 °C; (iii) a plane of InAs QDs with 3-monolayer coverage, deposited by Atomic Layer Molecular Beam Epitaxy (ALMBE) [25] at 460 °C. The structures have been grown both with and without a 20 nm-thick $In_xGa_{1-x}As$ upper confining layer (UCL); such a layer is grown by ALMBE at lower temperature (360 °C) in order to reduce the interaction among confining layers and QDs. The In content of LCLs and UCLs is identical and ranges from $x = 0.09$ to $x = 0.31$. Before and after the deposition of QDs, the growth has been interrupted for 210 s to change the substrate temperature. More details on the growth conditions can be found in reference [9]. The residual strain of MBs (LCLs) has been measured in structures with QDs in order to correlate the strain measurements done in this work to the emission energy studied by PL and reported in references [9,12,13].

Micro-Raman spectra have been measured with a Dilor LabRam system. In this set-up the excitation laser beam is sent to the sample through microscope optics. A HeNe laser light source ($\lambda = 632.8$ nm), with 15 mW laser power and a 100 magnification objective optics have been used. The Raman signal has been recorded by a silicon CCD camera cooled down to 210 K, with spectral resolution of 1 cm^{-1}. The spectra have been taken using 2 min integration times to improve the signal to noise ratio.

X-ray diffraction measurements have been performed by using a Philips high resolution diffractometer equipped with a four (220) reflections Ge-crystal monochromator for selecting the CuKα_1 X-ray radiation line. Reciprocal Space Maps (RSM) of the coherent scattered intensity have been obtained by using a triple bounce Ge crystal analyser scanning the reciprocal space with an angular resolution of 12 arcsec. In order to evaluate the strain relaxation of MB layers, RSMs around the asymmetrical (-224) and (2-24) have been used. The lattice parameters parallel and perpendicular to the interfaces and, then, the composition and the strain components have been obtained from the position in reciprocal space of the diffraction peaks due to the MB layer and the substrate [26]. Furthermore, linear $\omega - 2\theta$ scans (ω and θ being the incidence angles on the sample surface and on the scattering planes, respectively) through the asymmetrical 335 and symmetrical 004 reflections have been also collected for a selected number of structures in order to verify the occurrence of differences in the strain level of UCLs and LCLs. In this case advantage has been taken of the better signal-to-noise ratio of single scan measurements, as compared to the area scan (RSM) counterparts, related to the more favourable counting statistics.

3 Results and discussion

In Figure 1 the Raman spectra of the InAs/In$_{0.15}$Ga$_{0.85}$As structures with UCL in the frequency region of the GaAs-like longitudinal (LO) and transversal (TO) optical phonons are plotted. The structures related to InAs-like LO phonons are less intense and are not reported here. We note that the Raman frequency of our structures shifts
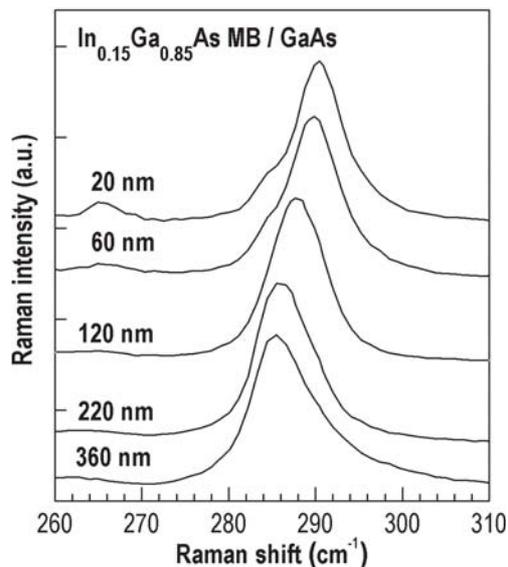
Fig. 1. Raman spectra of $In_{0.15}Ga_{0.85}As$ metamorphic buffers (MBs) of different thicknesses incorporated in InAs/InGaAs quantum dot nanostructures with GaAs substrates, in the spectral region of the GaAs-like LO phonon. Spectra are shifted vertically for clarity.

monotonically to lower values with increasing the LCL thickness, and the total shift is of ~ 5 cm^{-1} for t ranging from 20 to 360 nm. In the spectra we can also observe a less intense structure, which in the sample with $t = 20$ nm is around 265 cm^{-1}, due to the TO GaAs-like mode activated by disorder [16]. This structure shifts to lower frequencies and broadens with increasing t. The spectra have been carefully analysed in order to derive the peak energy of the GaAs-like LO mode by best fitting a Lorentzian lineshape to the experimental data. The resulting uncertainty in the value of the peak energy is 0.2 cm^{-1}.

According to references [16,19,27] a linear relation between the GaAs-like LO phonon frequency and the in-plane residual strain $\varepsilon = (a_{MB} - a_{InGaAs})/a_{InGaAs}$ of the InGaAs layer has been assumed. Here a_{MB} represents the lattice parameter of the MB in the growth plane, while a_{InGaAs} is the lattice parameter of free-standing $In_xGa_{1-x}As$ with the same x. In pseudomorphic InGaAs layers grown on GaAs, i.e. with thicknesses smaller than the critical thickness for plastic relaxation of the strain, a_{MB} coincides with the lattice parameter of free-standing GaAs.

The phonon frequency shift due to strain in the alloy layer is given by [19]:

$$\Delta\omega^{LO} = \omega^{LO} - \omega_0^{LO} = \left[\left(\frac{S_{12}K_{11}^{LO}}{S_{11} + S_{12}} + K_{12}^{LO} \right) \omega_0^{LO} \right] \varepsilon = \xi\varepsilon \tag{1}$$

where S_{ij} and K_{ij}^{LO} are the elastic compliance and phonon deformation potential tensors, respectively; ω^{LO} and ω_0^{LO} are the LO phonon frequency of strained and unstrained InGaAs, respectively.

In order to find the parameters of the linear dependence of ε on the measured ω^{LO} in $x = 0.15$ samples,

instead of relying on literature data for S_{ij}, K_{ij}^{LO} and ω_0^{LO} that are somewhat scattered we performed a best-fit of equation (1) by using the values of ω^{LO} from Raman measurements and of residual strain ε measured by means of photoreflectance (PR) measurements [11,24,28] on the same samples; this approach allow us to minimize the effects of unintentional differences among sample prepared by different techniques and under different conditions. Photoreflectance measurements yield the strain-related splitting between heavy- and light-hole bands at the Γ point of the Brillouin zone; according to the deformation potential theory [27,29]; such a splitting is linearly proportional to the in-plane strain.

The best-fit procedure yielded $\omega_0^{LO} = 285$ cm^{-1} and $\xi = -666.9$ cm^{-1} for $x = 0.15$. The value of ω_0^{LO} well compare with those measured in literature on strain-free InGaAs alloy layers [16].

We note that previously published PR results [24] for the same samples (with UCL) and similar samples without UCL, reported on the negligible variations observed in the parameter values of the HH and LH transitions, ensuring that UCLs are pseudomorphic to LCLs. Consequently, in the following, PR, Raman and XRD strain results will be equally well compared with theoretical predictions on strain relaxation.

Then ε values have been calculated by equation (1) with the above ξ and ω_0^{LO} parameters and experimental ω^{LO} values. These values are reported in Figure 2 as a function of the MB thickness; the figure also shows the ε values from RSM measurements in the vicinity of (224) reciprocal lattice nodes for structures with MBs with In composition in the 0.09–0.31 range, without UCLs and with QDs.

In Figure 3 we plot the reciprocal space map in the vicinity of (-224) reciprocal lattice node for the structure with In composition $x = 0.09$. The contours of constant scattered intensity around a node have been derived from a series of $\omega - 2\theta$ scans with different ω offsets. The conversion of each intensity-peak position $(\omega, 2\theta)$ in reciprocal space coordinates (Q_x and Q_z parallel to [-110] and [001], respectively) is given by [26]: $Q_x = R[\cos(2\omega') - \cos(2\omega' - \omega)]$ and $Q_z = R[\sin(\omega) - \sin(2\omega' - \omega)]$; where R is the Ewald sphere radius ($R = |\mathbf{k_i}| = 1/\lambda$) and $2\omega' = 2\theta_B$ when the Bragg condition is satisfied.

The broadening of the substrate and MB peaks are comparable along the reciprocal space [112] direction, thus demonstrating that strain (and composition) in MBs have not significant variations in depth. Instead, the much larger broadening of the MB intensity distribution perpendicular to [112] direction as compared to the substrate one is related to the "mosaicity" of MBs induced by the misfit dislocations intentionally formed to relax the elastic strain. The separation between the intensity maxima is directly related to the strain relaxation.

The values of ε in the range of plastic relaxation have been corrected by the so-called thermal misfit [30] Δ_T that is due to the different contraction of substrate and layer during cooling from the growth temperature T_g to
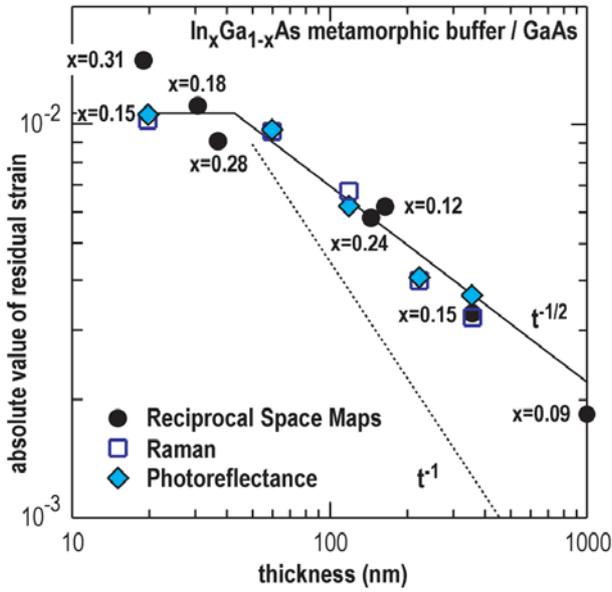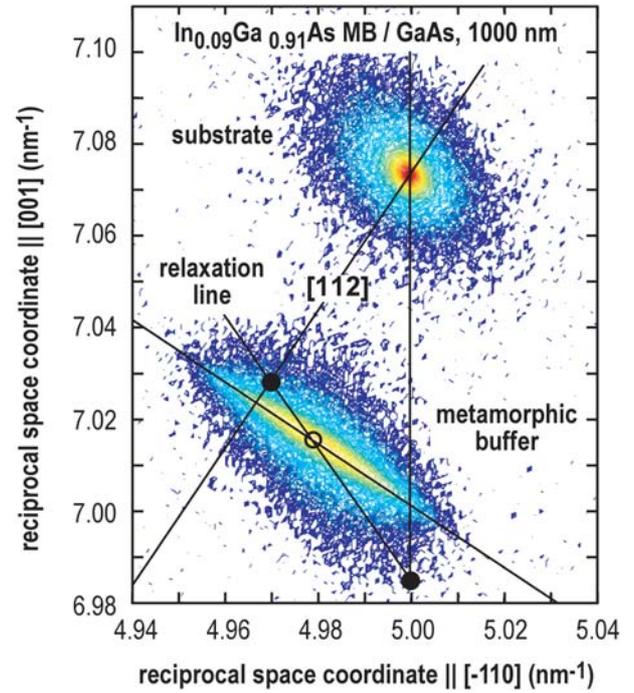
Fig. 2. Absolute value of residual in-plane strain ε as a function of the thickness t of $In_xGa_{1-x}As$ metamorphic buffers obtained by Raman scattering (open squares), reciprocal space map (RSM, closed circles), and photoreflectance (PR, closed diamonds) measurements. The continuous line shows the thickness dependence of strain both in the pseudomorphic regime (horizontal line, $x = 0.15$) and in the partial relaxation one where ε can be approximated by a $t^{-1/2}$ dependence [23]; the dotted line represents the t^{-1} behaviour foreseen by the equilibrium models [33–35]. Raman and PR measurements refer to $x = 0.15$ structures, while the MB compositions of structures for RSM are given in the figure.

Fig. 3. Reciprocal space map (RSM) around the -224 asymmetrical node of a structure consisting of a 1000 nm-thick $In_{0.09}Ga_{0.91}As$ metamorphic buffer (MB) and a GaAs substrate (broader and sharper diffraction peaks, respectively). The [112] crystallographic direction and its perpendicular (the mosaic broadening direction) are indicated. The relaxation line joining the reciprocal lattice nodes (black dots) associated to the full strained and full relaxed MB conditions is also shown. The open circle represents the position of the maximum of the buffer diffraction peak. The dashed line crossing the substrate and the full strained MB nodes is parallel to the [001] direction.

the room-temperature, under a condition where the defects can be considered as "frozen". The thermal misfit for the InGaAs/GaAs is definitely smaller than the value $\Delta_T = -3.76 \times 10^{-4}$ for $T_g = 490$ °C of the InAs/GaAs counterpart, that is calculated using the thermal expansion coefficients reported in the literature [31].

In Figure 2 we also report ε alues obtained by means of PR spectroscopy on the same samples [11,24]. We note that the strain values obtained by Raman scattering, X-ray diffraction and photoreflectance are in a very satisfactory agreement.

As for errors in the RMS measurements of the residual strain, we note that the occurrence of misfit dislocations at the substrate/buffer interface and the consequent sample curvature [32] result in the broadening of both substrate and buffer layer peaks (Fig. 3). The peak widening gives rise to a certain ambiguity in the determination of the angular position of the intensity maxima. This was particularly evident for the samples with thinnest MBs. Notwithstanding, the peak separation between the LCL and the substrate could be evaluated with an accuracy of ±30 arcsec, for which an error of ±1.5 × 10⁻⁴ in the calculated ε values was estimated. Concerning the MB composition x, the relative difference between the nominal and the values of the MB composition measured by X-ray diffraction is always less than 5% and the estimated

error is ∼±2.5%, except for one case where it was ±4.0%. The reported composition of samples measured by Raman scattering and PR are the nominal ones, very close to those measured by XRD techniques.

As regards the Raman measurements, the uncertainty of 0.2 cm⁻¹ in the peak energy ω_{LO} yields an error in the determination of ε values that is ±2 × 10⁻⁴.

Let us compare now our experimental results with predictions of existing models of strain relaxation. It is well-known that when the critical thickness is exceeded the epitaxial growth of a lattice mismatched layer is no longer pseudomorphic. The lattice mismatch is accommodated partly by elastic strain and partly by the formation of a misfit dislocation network. In the frame of the continuum elasticity theory the equilibrium between elastic and plastic accommodation is found by minimizing the total energy of the system [33], given by the elastic strain energy and the dislocation energy. The models based on this assumption, lead to a strain relaxation rate proportional to t^{-1}, where t is the epilayer thickness [33,35]. Most of the experimental observations made on different epitaxial systems, indicate that while the equilibrium models quite properly give the critical thickness for the onset of

the formation of misfit dislocations, they cannot explain the strain relaxation rate as well. If the energy-balance model [23] is assumed, the relation $\varepsilon^2\, t \sim$ const. is obtained, that gives a $\sim t^{-1/2}$ dependence for the residual strain. Figure 2 shows that the experimental values of ε obtained by both Raman scattering and X-ray diffraction experiments, as well as by PR, are in better agreement to the prediction of the model of Marée et al. than with those of references [33–35], thus producing further support to former model of strain relaxation in mismatched materials.

The former model [23] considers the nucleation and expansion of dissociated half loop dislocations originating from the free surface of the layer and propagating down to the interface between layer and substrate. The assumption is that the energy of the half loop system increases during the expansion until a critical loop radius is achieved where the energy is a maximum. Then, the expansion continues lowering the total energy of the system.

Raman measurements performed on structures with $t = 220$ nm and higher composition (not reported here) have revealed well-behaved LO phonon spectral features also for $x = 0.35$. This indicates the possibility to optically determine the strain status even when it cannot be obtained through PR measurements. Indeed it has been shown that PR determination of strain stems from the accurate measurement of the splitting between the LH- and HH-related interband transitions: this procedure may be hindered by the broadening of optical transitions which increases with increasing In composition. On the other hand, Raman measurements of residual strain can be done provided that the proportionality constants between ω^{LO} shift and ε are known for the alloy composition of interest, either from the literature or from calibrations, as it has been done in the present paper.

It should be noted that the values of ω^{LO} of strained $In_xGa_{1-x}As$ depend not only on the values of the residual strain ε but also on the material composition x. Therefore any uncertainty on x affects the accuracy of the measurement of ε. On the other hand, XRD measurements simultaneously and directly give x and ε, without the need of any calibration with other techniques, but — as a drawback — are much more time-consuming than the Raman characterization of residual strain. It is useful to remind that results of the PR approach to measure strain are fairly independent of layer composition, since ε is deduced from the difference of two quantities (the HH and the LH energy gaps) that present a similar dependence on x.

From the analysis of the $\omega - 2\theta$ scans, structures with and without UCL on top of QDs show no significant differences in the strain status. An exception is made for a structure with $x = 0.31$ and a 19-nm thick LCL, that — for reasons under investigation — showed an anomalously high density of threading dislocations in Transmission Electron Microscopy (TEM) cross-sections. Moreover, in references [24] and [28] it was shown by PR measurements of the same structures studied in the present work that negligible differences exists between the in-plane strain in structures with and without UCLs, thus confirming that

UCLs are pseudomorphic to LCLs. Hence, the comparison presented in Figure 2 between the results obtained in structures with and without UCL is justified and the assumption of the model developed to calculate the light emission energy from strain-engineered QD InAs/InGaAs nanostructures [9] is substantiated.

4 Conclusions

In order to study the strain relaxation of constant-composition metamorphic buffers as a function of their thickness, we have considered two well known techniques to determine quantities linearly dependent on the in-plane residual strain ε of an epitaxial layer grown on a mismatched substrate. Those are Raman scattering, that gives the LO phonon frequency ω^{LO} of the strained material, and X-ray diffraction either in the Reciprocal Space Map and in the single $\omega - 2\theta$ scan modes, that directly yields the values of lattice parameter a_{MB} of the metamorphic buffer and, then, of ε. The ε-vs.-ω^{LO} working curve for Raman measurements has been obtained by fitting the Raman shift data to the values of the residual strain deduced by photoreflectance on the same samples. We have shown that the ε values measured by means of Raman, XRD and PR are in a very satisfactory agreement and the respective advantages of the techniques are discussed.

The residual strain values ε versus the thickness t of metamorphic buffers have been compared to the results of strain relaxation models, that give different $\varepsilon(t)$ dependences; the experimental data confirm the validity of the energy-balance model [23] that foresees an approximate $t^{-1/2}$ dependence.

These results are of great interest in designing metamorphic epitaxial structures where the strain induced by buffer layers can be used as a tool to modify in a predictable way the electronic band structure of the upper layers. An interesting example is the QD strain engineering [9,12] of InAs/InGaAs QD nanostructures grown on GaAs substrates, that results in the shift of the RT light emission wavelength towards the 1.55 μm spectral window of telecom and datacom applications.

In addition, the knowledge of the mechanism that determine the strain relaxation may allow the design of advanced heteroepitaxial structures, where graded-composition MBs are incorporated to take specific advantages over the constant-composition counterparts, as regards the confinement of misfit dislocations far away from the active region of the structures [14].

References

1. *Properties of Lattice-matched and Strained Indium Gallium Arsenide*, edited by P. Bhattacharya (Inspec, London, 1993)
2. F.H. Pollak, in *Semiconductors and Semimetals*, edited by T.P. Pearsall (Academic, London, 1990), Vol. 32, p. 17
3. W.E. Hoke et al., J. Vac. Sci. Technol. B **17**, 1131 (1999)
4. O. Baklenov et al., J. Vac. Sci. Technol. B **20**, 1200 (2002)
5. F. Dimroth, U. Schubert, A.W. Bett, IEEE Electron Device Lett. **21**, 209 (2000)
6. G. Abstreiter, H. Brugger, T. Wolf, H. Jorke, H.J. Herzog, Phys. Rev. Lett. **54**, 2441 (1985)
7. E.A. Fitzgerald, Materials Science and Engineering B **124**–**125**, 8 (2005)
8. Y.C. Xin, L.G. Vaughn, L.R. Dawson, A. Stintz, Y. Lin, L.F. Lester, D.L. Huffaker, J. Appl. Phys. **94**, 2133 (2003)
9. L. Seravalli, M. Minelli, P. Frigeri, P. Allegri, V. Avanzini, S. Franchi, Appl. Phys. Lett. **82**, 2341 (2003)
10. A.E. Zhukov, A.P. Vasil'ev, A.R. Kovsh, S.S. Mikhrin, E.S. Semenova, A.Yu. Egorov, V.A. Odnoblyudov, N.A. Maleev, E.V. Nikitina, N.V. Kryzhanovskaya, A.G. Gladyshev, Yu.M. Shernyakov, M.V. Maximov, N.N. Ledentsov, V.M. Ustinov, Zh.I. Alferov, Semiconductors **37**, 1411 (2003)
11. M. Geddo, V. Bellani, G. Guizzetti, M. Patrini, T. Ciabattoni, L. Seravalli, M. Minelli, P. Frigeri, S. Franchi, *Electrochemical Society Proceedings* (2005), Vol. 2004-13, p.373
12. L. Seravalli, P. Frigeri, M. Minelli, P. Allegri, V. Avanzini, S. Franchi, Appl. Phys. Lett. **87**, 063101 (2005)
13. L. Seravalli, P. Frigeri, M. Minelli, P. Allegri, V. Avanzini, S. Franchi, Materials Science Engineering C **26**, 731 (2006)
14. A. Bosacchi, A.C. De Riccardis, P. Frigeri, S. Franchi, C. Ferrari, S. Gennari, L. Lazzarini, L. Nasi, G. Salviati, A.V. Drigo, F. Romanato, J. Cryst. Growth **175**–**176**, 1009 (1997)
15. F. Calle, A. Sacedon, A.L. Alvarez, E. Calleja, E. Muño, H.G. Colson, P. Kidd, Microel. Journal **26**, 821 (1996)
16. J. Groenen, G. Landa, R. Carles, P.S. Pizani, M. Gendry, J. Appl. Phys. **82**, 803 (1997)
17. O. Brafman, D. Fekete, R. Safarty, Appl. Phys. Lett. **58**, 400 (1991)
18. M.F. Whitaker D.J. Dunstan, J. Phys. Condens. Matter **11**, 2861 (1999)
19. H.K. Shin, D.J. Lockwood, C. Lacelle, P.J. Poole, J. Appl. Phys. **88**, 6423 (2000)
20. K. Ishida, J. Mtsui, T. Kamejima, I. Sakuma, Phys. Status Solidi (a) **31**, 255 (1975)
21. P.F. Fewster, Semicond. Sci. Technol. **8**, 1915 (1993)
22. Yu.P. Khapachev, F.N. Chukhovskii, Sov. Phys. Crystallogr. **34**, 465 (1989)
23. P.M.J. Marée, J.C. Barbour, J.F. Van der Veen, K.L. Kavanagh, C.W.T. Bulle-Lieuvma, M.V.A. Viegers, J. Appl. Phys. **62**, 4413 (1987)
24. M. Geddo, G. Guizzetti, M. Patrini, T. Ciabattoni, L. Seravalli, P. Frigeri, S. Franchi, Appl. Phys. Lett. **87**, 263120 (2005)
25. ALMBE is a variant of MBE where group-III and group-V species impinge on the substrate alternatively in monolayer or sub-monolayer amounts per cycle
26. P.F. Fewster, Appl. Surface Sci. **50**, 9 (1991)
27. B. Jusserand, M. Cardona, in *Light Scattering in Solids V*, Topics in Applied Physics, edited by M. Cardona, G. Güntherodt (Springer, New York, 1989), Vol. 66, p. 49
28. L. Seravalli, M. Minelli, P. Frigeri, S. Franchi, G. Guizzetti, M. Patrini, T. Ciabattoni, M. Geddo, J. Appl. Phys. **101**, 024313 (2007)
29. F.H. Pollak, M. Cardona, Phys. Rev. B **172**, 816 (1968)
30. C. Bocchi, A. Bosacchi, S. Franchi, S. Gennari, R. Magnanini, A.V. Drigo, Appl. Phys. Lett. **71**, 1549 (1997)
31. *Landolt-Börnstein Numerical Data and Functional Relationships in Science and Technology*, edited by O. Madelung, M. Schultz, H. Weiss, New series (Springer, Berlin, 1982), Vol. 17
32. C.R. Wie, in *Properties of Lattice-matched and Strained Indium Gallium Arsenide,* edited by P. Bhattacharya (Inspec, London, 1993), p. 257
33. J.W. Matthews, A.E. Blakeslee, J. Crystal Growth **27**, 118 (1974)
34. D.J. Dunstan, Philos. Mag. A **73**, 1323 (1996)
35. D.J. Dunstan, P. Kidd, L.K. Howard, R.P. Dixon, Appl. Phys. Lett. **59**, 3390 (1991)